PAPER • **OPEN ACCESS**

Numerical analysis of AISI 321 alloy material parameters on rubber pad diaphragm forming

To cite this article: P S Barros *et al* 2022 *IOP Conf. Ser.: Mater. Sci. Eng.* **1238** 012005

Numerical analysis of AISI 321 alloy material parameters on rubber pad diaphragm forming

P S Barros[1,2*], N Otegi[1], L Galdós[1] and E Sáenz de Argandoña[1]

[1] Mondragon Unibertsitatea, Loramendi Kalea, 4, 20500 Mondragon, Spain
[2] ITP-Aero, Parke Tecnológico de Bizkaia, Edificio 902, 48160 Derio, Spain

* psanchez@mondragon.edu

Abstract. Rubber pad diaphragm forming is a technology that uses a rigid die in conjunction with a flexible polyurethane tool and fluid pressure action in order to shape metal sheets. In this process, the action of the fluid forms a polyurethane tool, which forces the sheet to acquire the geometry of the die, being this process quite different from the classical stamping processes. The rubber tool is compatible with different die geometries, which allows a quick reconfiguration of the system, making it adequate for the production of small batches in the aeronautical sector. In this study, an advanced numerical model of the process is developed, in order to obtain a simulation that allows comprehensive understanding of the technology. An advanced characterization of the AISI 321 stainless steel is carried out, evaluating different yielding criteria. On the other side, the hyperelastic behaviour of the polyurethane rubber is taken into account. The main goal of the study has been to perform a sensitivity analysis of the sheet material parameters and to understand their influence on the final numerical results.

1. Introduction

Nowadays the use of numerical methods and finite elements is more widespread in the daily use of the industry. The numerical simulations, allows the companies to reduce the designing time, the try outs and consequently the costs, increasing the competitiveness of the industries. In the field of sheet metal forming processes, simulation plays a fundamental role, allowing us to detect the defects, before forming the blanks. This detection of defects is important in industries such as the aeronautical industry, where despite small size of the batches, the presence of defects in the parts, like earing, splits, wrinkles and springback or a high number of try outs, supposes a loss of competitiveness. In order to avoid this problem, it is important to understand which ones are the main control variables in the process and in the simulation.

This work will focus on the rubber pad diaphragm forming process, a rubber forming process introduced in the industry in the last years, and based on the Verson-Wheelon process [1]. This process was designed with the aeronautical industry in mind, since it allows the production of small batches and a relatively fast die exchange. As its name indicates, the process is framed within the rubber forming processes, being the simulation field of this type of technology less developed. Different elements are used in the rubber pad diaphragm forming process. On the one hand, it is a die with the geometry that it is desired to obtain. The sheet metal is placed on this die, and on the blank, a rigid rubber tool known as throw pad is placed. The machine contains a volume of oil, which is supported by a soft rubber diaphragm. To perform the forming, the pressure is increased in the oil,

which deforms the diaphragm like a balloon, and pushes the other elements in a similar way to the hydroforming process.

In order to better understand the influence of the characterization of the sheet material on the process, different yield criteria will be evaluated by finite element simulation. In this work, the yield constitutive models that will be fitted and simulated are, the Hill48's criterion, proposed by R.Hill in 1948 [2], being one of the simplest and more used in sheet metal forming simulation, the Yld-2000's criterion, proposed by F.Barlat et al. in 2003 [3] and the 6th order Yoshida's criterion, proposed by Yoshida et al. in 2013 [4].

To carry out this study, the metallic stainless steel alloy AISI 321 will be used. This kind of alloy was selected for its use in the aeronautical industry, as well as its good mechanical properties and formability [5]. In this work, the throw pad will also be introduced, and its hyperelastic mechanical behavior will be described [6]. The selected material for the rubber will be a polyurethane rubber with ShoreA 90 hardness and 10 mm thickness. In order to evaluate the influence of the mechanical properties of the AISI 321 in the process, a battery of simulations will be carried out in which different frictions and yield criteria will be mixed, in order to see which one of the variables has a greater influence on the process.

2. Materials and methods

2.1. Constitutive material laws

The AISI 321 blank mechanical behavior during the forming process is described in the numerical simulation by the constitutive models. The elastic behavior of the material is defined by its Young's modulus E and the Poisson's coefficient υ. The material hardening defines the stress-strain relation when the material is in the plastic regime and the yield criterions, sets the boundaries between the elastic and plastic regimes, determined by the yield stress σ_y. The yield criteria compared in this article, are given by:

- Hill's criterion (1948) [2]: Extended the Von Mises criterion, introducing stress weighting coefficients in each direction, in order to take into account the anisotropy of the material, where F, G, H, L, M, N are constants to be defined by experimental tests. It is a symmetric and quadratic criterion in shape. These coefficients are generally calculated starting from the anisotropy coefficients (r) at 0°, 45° and 90° from the rolling direction. This criterion is widely used and provide good results in the simulation of steel materials.

$$F(\sigma_{22}-\sigma_{33})^2 + G(\sigma_{33}-\sigma_{11})^2 + H(\sigma_{11}-\sigma_{22})^2 + 2L{\sigma_{23}}^2 + 2M{\sigma_{31}}^2 + 2N{\sigma_{12}}^2 = 2{\sigma_y}^2 \quad (1)$$

The previous equation is used for describe the three-dimensional yield behaviour; however, as in metal forming the work material are sheets, we can remove the thickness components in order to work with a bi-dimensional criteria.

$$(H+F)(\sigma_{22})^2 + (G+H)(\sigma_{11})^2 - 2H\sigma_{11}\sigma_{22} + 2N{\sigma_{12}}^2 = 2{\sigma_y}^2 \quad (2)$$

- Yld-2000's criterion (2003) [3]: In order to improve their 1991 and 1994 criteria, Barlat et al. propose this new criterion, which aims to reduce the complexity of their previous models, but without losing flexibility. This yield criterion, uses eight coefficients, in order to describe the yield surface [7].

$$X = X' + X'' = 2{\sigma_y}^M \quad (3)$$

$$\left.\begin{cases} X' = \left|X'_1 - X'_2\right|^M \\ X'' = \left|2X''_2 + X''_1\right|^M + \left|2X''_1 + X''_2\right|^M \end{cases}\right\}; \left\{\begin{cases} X'_i = \frac{1}{2}\left(X'_{11} + X'_{22} \pm \sqrt{(X'_{11}-X'_{22})^2 + 4X'^2_{12}}\right) \\ X''_j = \frac{1}{2}\left(X''_{11} + X''_{22} \pm \sqrt{(X''_{11}-X''_{22})^2 + 4X''^2_{12}}\right) \end{cases}\right\} \quad (4)(5)$$

$$\left\{ \begin{matrix} \boldsymbol{X}^{'} = \boldsymbol{L}^{'}\boldsymbol{\sigma} \\ \boldsymbol{X}^{''} = \boldsymbol{L}^{''}\boldsymbol{\sigma} \end{matrix} \right\} \tag{6}$$

$$\begin{bmatrix} L'_{11} \\ L'_{12} \\ L'_{21} \\ L'_{22} \\ L'_{66} \end{bmatrix} = \begin{bmatrix} 2/3 & 0 & 0 \\ -1/3 & 0 & 0 \\ 0 & 0 & 0 \\ 0 & -1/3 & 0 \\ 0 & 2/3 & 1 \end{bmatrix} \begin{bmatrix} \alpha_1 \\ \alpha_2 \\ \alpha_7 \end{bmatrix} ; \begin{bmatrix} L''_{11} \\ L''_{12} \\ L''_{21} \\ L''_{22} \\ L''_{66} \end{bmatrix} = \begin{bmatrix} -2 & 2 & 8 & -2 & 0 \\ 1 & -4 & -4 & 1 & 0 \\ 4 & -4 & -4 & 4 & 0 \\ -2 & 8 & 2 & -2 & 0 \\ 0 & 0 & 0 & 1 & 9 \end{bmatrix} \begin{bmatrix} \alpha_3 \\ \alpha_4 \\ \alpha_5 \\ \alpha_6 \\ \alpha_8 \end{bmatrix} \tag{7)(8}$$

- Yoshida's criterion (2013) [4]: This criterion, developed by Yoshida et al. uses a sixth-order polynomial yield function, in order to describe the yielding surface of the material. The Yoshida's criterion, uses sixteen anisotropy coefficients. Thanks to the amount of coefficients, this criteria proves good flexibility to adjust the experimental points. On the other side, the drawback of the Yoshida's criterion is the number of experimental points that should be obtained in order to fit the model. The model needs at least sixteen experimental points to be fitted.

$$C_1{\sigma_{11}}^6 - 3C_2{\sigma_{11}}^5\sigma_{22} + 6C_3{\sigma_{11}}^4{\sigma_{22}}^2 - 7C_4{\sigma_{11}}^3{\sigma_{22}}^3 + 6C_5{\sigma_{11}}^2{\sigma_{22}}^4 - 3C_6\sigma_{11}{\sigma_{22}}^5 + C_7{\sigma_{22}}^6 + 9\big(C_8{\sigma_{11}}^4 - 2C_9{\sigma_{11}}^3\sigma_{22} + 3C_{10}{\sigma_{11}}^2{\sigma_{22}}^2 - 2C_{11}\sigma_{11}{\sigma_{22}}^3 + C_{12}{\sigma_{22}}^4\big){\sigma_{12}}^2 + 27\big(C_{13}{\sigma_{11}}^2 - C_{14}\sigma_{11}\sigma_{22} + C_{15}{\sigma_{22}}^2\big){\sigma_{12}}^4 + 27C_{16}{\sigma_{12}}^6 = {\sigma_y}^6 \tag{9}$$

In the case of the material hardening, the tensile test provides experimental data of the stress-strain relation between the yield stress and the ultimate strength of the material. In order to extrapolate this behaviour to bigger deformations, different hardening models exists. In this study only one model will be used, the Hollomon's hardening law, a simple isotropic hardening model, widely use in the practice. This model is given by:

- Hollomon's hardening law (1945) [8]: The Hollomon's hardening equation is a power law that defines a relation between the true stress and the true strain. In this equation K is the strength coefficient, and n is the strain hardening exponent.

$$\sigma(\varepsilon) = K\,\varepsilon^n \tag{10}$$

The ShoreA 90 polyurethane rubber it is characterized by its hyperelastic behaviour. The hyperelasic material behaviour is defined by the Green's theory. Unlike linear elasticity, where the relationship between stress and strain is obtained directly, in this case the relationship is derived from an energy potential function [9]. One of the most used hyperelastic models was set by R.S. Rivlin and proposes the following formulation for the potential energy equation:

- Mooney-Rivlin (1948) [10]: The Mooney-Rivlin model is typically used in the modelling of rubber tools in rubber forming processes numerical simulation. In this model, the values of C_{10} and C_{01} are material dependent constants and I_1 and I_2 the first and second invariants of the strain tensor.

$$\boldsymbol{\sigma} = \partial W/\partial \boldsymbol{\varepsilon} \quad ; \quad W(I_1, I_2) = C_{10}(I_1 - 3) + C_{01}(I_2 - 3) \tag{11)(12}$$

2.2. Parameter identification

The characterized materials will be, on the one hand, the austenitic stainless steel AISI 321, in a 0.76 mm thick sheet format, and on the other hand, the thermoplastic polyurethane with a Shore A 90 hardness with a thickness of 10 mm. To carry out all the tests, the equipment used was a universal testing machine. In the case of the AISI 321 alloy, the tests used have been tensile tests at different angles of the rolling direction, as well as plane strain tests, simple shear tests and stack compression tests. In the case of polyurethane, only uniaxial tensile tests have been performed. The strain rate obtained for the samples in all the test were 0.016 s^{-1} approximately. A summary of the experimental results can be seen in the Table 1.

Table 1. Experimental points for the yielding fitting

Test	*Sample angle [º]*	*Normalize yield stress [-]*	*Lankford Coefficient [-]*
Uniaxial	0	1.000	0.505
Uniaxial	15	0.978	0.637
Uniaxial	30	0.970	0.813
Uniaxial	45	0.935	0.951
Uniaxial	60	0.968	0.917
Uniaxial	75	1.005	0.721
Uniaxial	90	1.002	0.637
Plane strain	0	1.058	-
Plane strain	90	1.085	-
Simple shear	45	0.573	-
Stack compression	-	-	0.744

2.2.1. Uniaxial tensile test. To carry out the tensile tests, tensile specimens have been cut every 15º with respect to the rolling direction of the original steel blank. For the measurement of the deformations and strains, a digital image correlation (DIC) system has been used.

2.2.2. Plane strain test. For the design of the geometries used in this study, the starting point for the geometries have been the designs used by other authors, such as G. Gruben et al. [11] and K. Zang et al. [12]. The final geometry is described in Figure 2. Starting from the previously mentioned geometries, a modification has been done to them, in order to adapt the test to the conditions that exist in the case of the equipment and material. These variations in geometry have been validated by finite element simulation, with the material properties previously obtained from the uniaxial test. In this way, the desired state of charge has been obtained. The test of the plane strain specimens was carried out on specimens cut at 0º and at 90º with respect to the rolling direction. In order to ensure the deformation state during the test, the strain was measured by DIC.

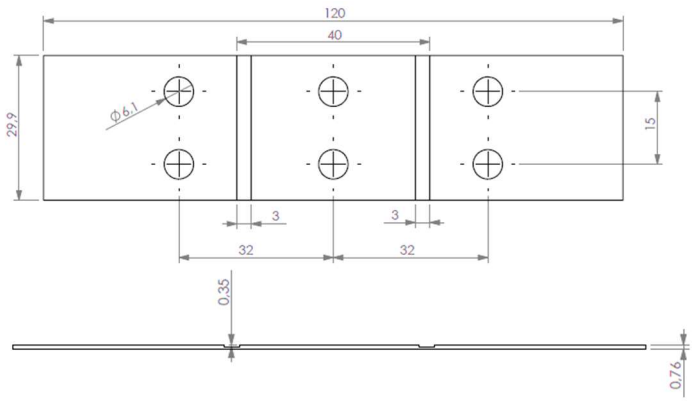

Figure 1. Sample geometry used for simple shear tests

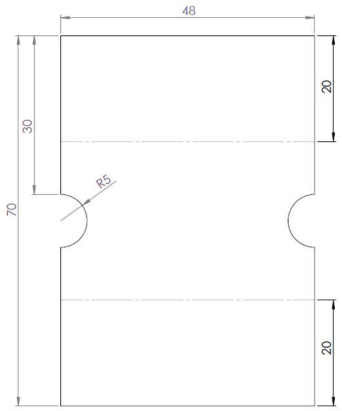

Figure 2. Sample geometry used for plane strain test

2.2.3. Stack compression test. In order to determine the $r_{biaxial}$, the stack compression test will be used. The process followed is described by Barlat et al. [3] in their work that describes the characterization of an aluminium alloy. In order to obtain a sample with the necessary high, fourteen blanks have been stacked, with a total thickness of 10.64 mm and then a diameter of 7.5 mm was cut using EDM. The experimental points were obtained under reductions in thickness of 4 mm, 5 mm and 6 mm.

2.2.4. Simple shear test. The shear test had been performed following the methodology described by M.Abspoel et al. [13], but measuring the deformations by DIC. The test was carried out with the sample at 45º respect to the rolling direction, in order to obtain the yield stress point with $\sigma_{xx}= \sigma_{yy}$ and $\tau_{xy}=0$. In the tooling, the central part of the sample, described in the Figure 1, has vertical movement and the side parts are fixed, reaching the simple shear state in the regions in between.

2.2.5. Material parameter fitting. In order to determine the parameters of the different yield criteria, the strategy followed was to minimize the error between the experimental parameters from the Table 1 and the values provided by the different models. The results of the fitting process of the yield criteria are exposed in the Table 2, and the comparison between the different models can be appreciated in the Figure 4. The error formulation used, was proposed by the members of the CERTETA research group [7], being d the distance between the experimental points, and its projection in the predicted yield locus :

$$\beta = \varphi + \delta + \gamma \quad (13)$$

$$\varphi = \sqrt{\sum_{i=1}^{n}(d^2)}\frac{1}{Y}\,100 \quad ; \quad \delta = \sqrt{\sum_{i=1}^{n}\left(\frac{\sigma_{\theta i}^{exp}-\sigma_{\theta i}^{t}}{\sigma_{\theta i}^{exp}}\right)}\,100 \quad ; \quad \gamma = \sqrt{\sum_{i=1}^{n}\left(\frac{r_{\theta i}^{exp}-r_{\theta i}^{t}}{r_{\theta i}^{exp}}\right)}\,100 \quad (14)(15)(16)$$

Table 2. AISI 321 yield parameters

Yoshida	C_1	C_2	C_3	C_4	C_5	C_6	C_7	C_8	C_9	C_{10}
	1	0.591	0.846	1.129	1	0.737	0.930	1.055	0.966	1.464
	C_{11}	C_{12}	C_{13}	C_{14}	C_{15}	C_{16}	-	-	-	-
	1.024	1.030	1.186	1.780	1.225	1.698	-	-	-	-
Yld 2000	α_1	α_2	α_3	α_4	α_5	α_6	α_7	α_8	M	-
	1	0.938	1.2	1.041	1.087	1.292	1.066	0.985	8	-
Hill 48	F	G	H	N	-	-	-	-	-	-
	0.527	0.664	0.336	1.734	-	-	-	-	-	-

On the other side, in order to fit the Hollomon hardening model, the procedure used was the minimization of the sum of existing relative errors, between the points obtained experimentally and the points provided by the Hollomon model. The obtained results are detailed in Table 3 and Figure 3.

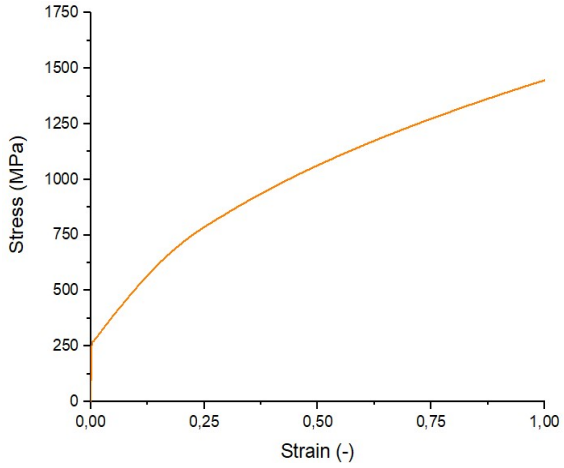

Figure 3. AISI 321 hardening curve

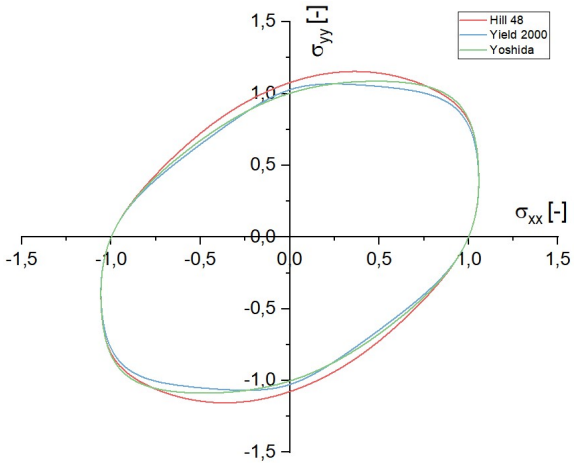

Figure 4. Yield surfaces comparison

Table 3. AISI 321 hardening parameters

	K [MPa]	*n [-]*
Hollomon	1446.64	0.443

2.2.6. Rubber uniaxial test. For the rubber characterization, uniaxial tension and compression tests were performed. The rubber samples were cyclically loaded and unloaded five times, due to its hysteresis softening. In the fifth cycle, the behaviour of the rubber stabilizes. This process is repeated under different deformations, in order to obtain a set of points that were used to fit the Mooney-Rivlin model. The coefficients obtained were C_{10}=1.06 MPa and C_{01}=0.87 MPa, assuming the incompressibility of the rubber.

3. Finite elements model

In order to carry out the analysis, the software "Pam-Stamp Professional 2021.0" has been used. The model that is used can be appreciated in the Figure 5. In this model, the die is defined as a rigid shell, on which the metal sheet is placed, with the material properties obtained from the previously described tests and constitutive models, and also described as a shell. In the case of rubber, it is placed on the sheet, and it is considered that the pressure from the machine is applied uniformly over the entire upper surface of the rubber pad. The rubber is defined using solid elements. Finally a double symmetry is applied in the die in order to reduce the computation time.

The friction is described as constant and between each pair of objects. In the case of the coefficient of friction (COF) between the blank and the die, the values would be 0.05 and 0.1, as it seems to be the limiting values of the friction, obtained after the strip drawing test. In the case of the rubber friction, the values of the coefficient of friction is obtained from bibliography, from the work of R.Elleuch et al [14]. The values of the rubber COF will be 0.5 and 0.4, in order to understand the influence of this variable in the process. The geometry of the sample is based in the geometries that are produced for the aeronautic industry, and the forming pressure used is 80 MPa.

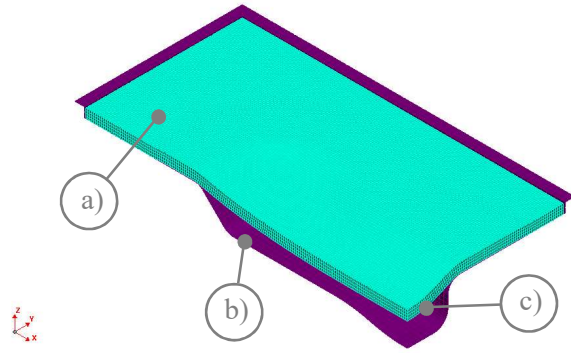

Figure 5. Rubber pad diaphragm forming simulation model a) Blank ; b)Rubber ; c) Die

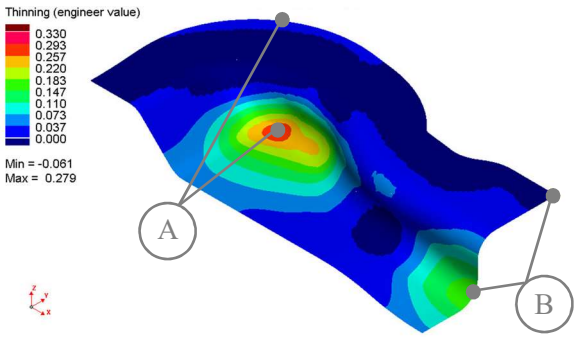

Figure 6. Points used to evaluate thinning, draw-in and springback. Thinning results using Hill 48 model, with blank COF 0.05 and rubber COF 0.4.

Two regions were selected in order to carry out the study, these regions can be seen in the Figure 6. The points used to evaluate the thinning are the two locations that present the maximum value of this parameter. In the case of the springback and the draw-in, the selected points are located in the flange points that are associated with the maximum thinning areas.

4. Results and discussion

The results obtained in the different numerical models, can be appreciated in the Figure 7. In a first sight, the differences in the results provided by all the models can be clearly seen, being the differences smaller between the Yld-2000 and Yoshida's model. The influence of each of the study variables on the results is described below.

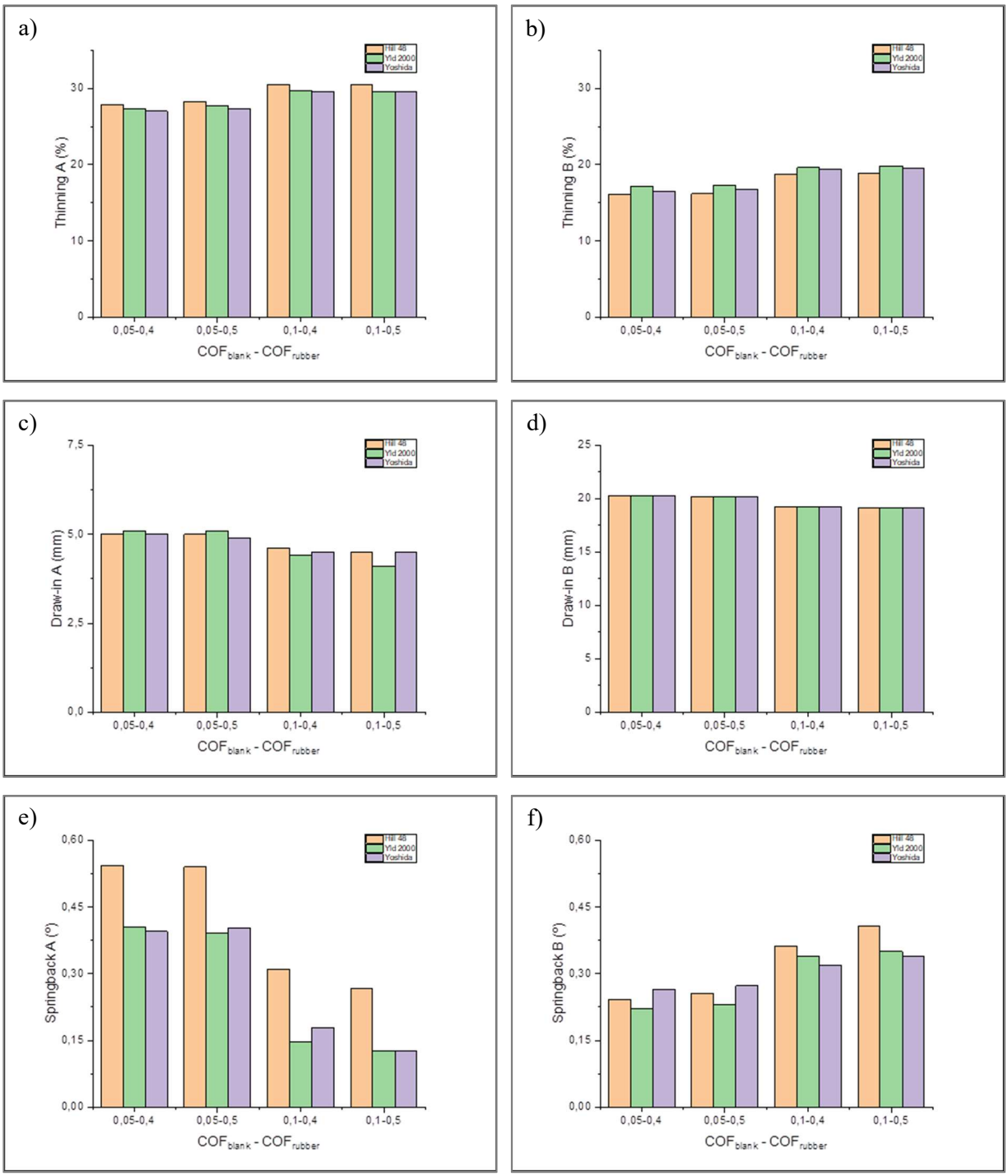

Figure 7. Results of the simulated geometry a) Maximum thinning A ; b) Maximum thinning B ; c) Draw-in A ; d) Draw-in B ; e) Springback A ; f) Springback B

In view of the results, in order to analyse the influence on the one hand of friction, as well as on the other hand of the material model, a factorial analysis has been carried out with the available data. In order to perform the analysis, the material model and the COF in the blank has been taken as control variables, and the COF in the rubber, due to its low influence, and the difficulty to control it in the process, has been taken as noise variable. The analysis is done at each point for each study parameter.

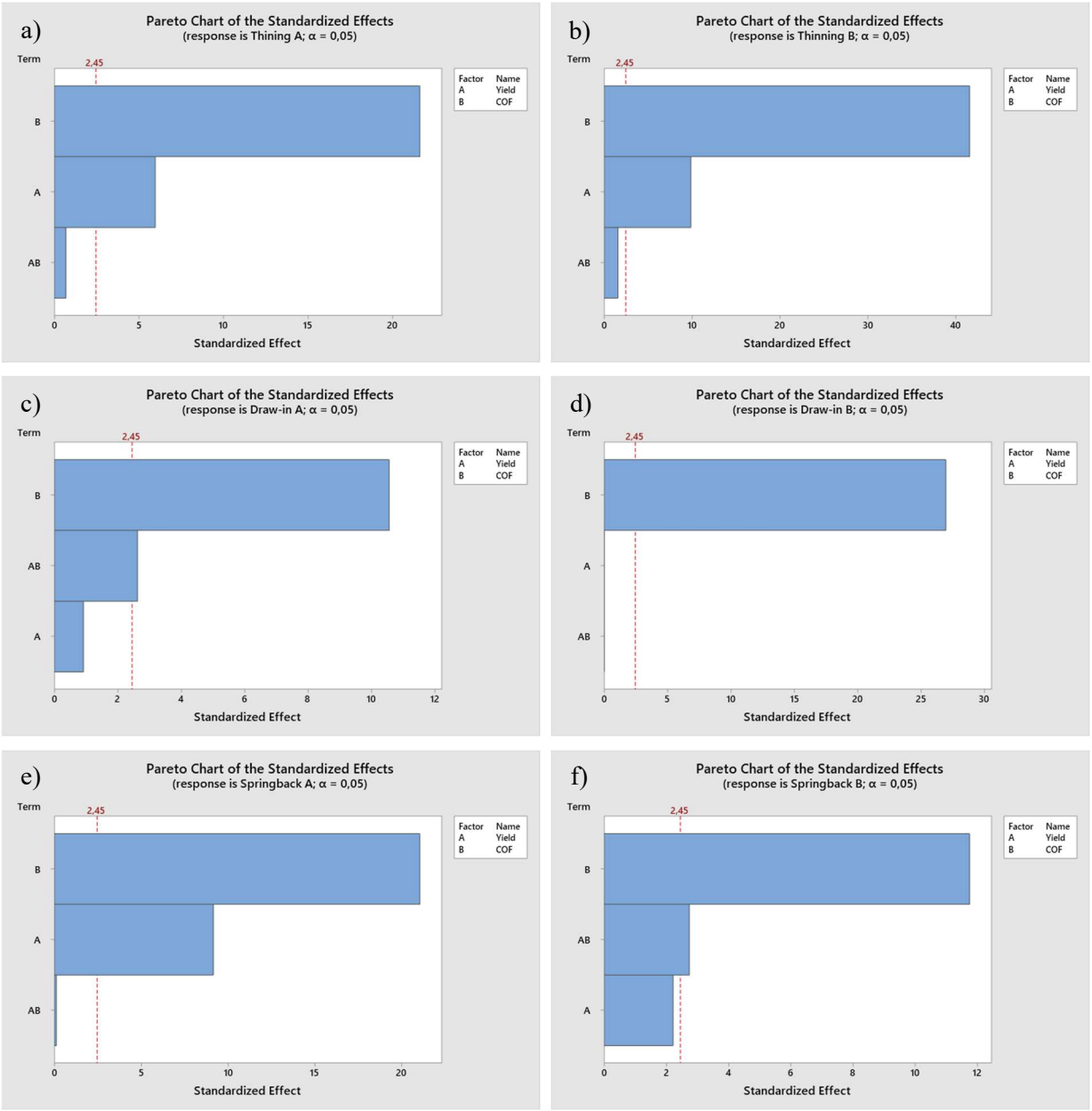

Figure 8. Pareto charts of the factorial analysis a) Maximum thinning A ; b) Maximum thinning B ; c) Draw-in A ; d) Draw-in B ; e) Springback A ; f) Springback B

In the case of thinning, the main variable that would produce variations in it would be the coefficient of friction, followed by the model of the material, and both having an influence that would not be negligible and as can be seen, there would be hardly any influence of the interaction between both.

On the other hand, looking at the draw-in of the blank at the end of the process, this could be considered to be controlled only by the friction between the sheet and the die, this can be seen in the results of the Figure 7 b).

Finally, in the case of springback, this is mostly influenced by the coefficient of friction, however, to a lesser extent, an additional variability arises, conditioned by the yield model used in the material. As can be seen, the main variable that controls the variability of the process is the coefficient of friction, however, the differences that arise in the results due to the use of a yield criterion or another cannot be ignored.

5. Conclusions

In the range of variables studied, the most relevant element is the coefficient of friction then the material model, and finally the friction coefficient of the rubber. The main conclusions that can be drawn from this analysis are, on the one hand, the importance of the control of the friction coefficient and the lubrication in production, in order to reduce the variability of the process. In addition, for modelling, having an adequate characterization of the friction in the process, as well as an adequate characterization of the material.

As future works, a correlation should be carried out with real manufactured parts, in order to determine which material model fits better the material AISI 321 in this process, and perform a complete sensitivity analysis with all the process variables.

6. Acknowledgements

It has been possible to carry out this study, thanks to the collaboration of ITP Aero. This work was supported in part by the Basque Government's R&D program Hazitek under Grant ZE-2020/0000.

References

[1] Z M Ramezani 2012 *Rubber-pad forming processes: Technology and applications* 1st ed. Woodhead Publishing
[2] R Hill 1948 *Proceedings of the Royal Society of London. Series A. Mathematical and Physical Sciences* **193** 281–97
[3] F Barlat, J C Brem, J W Yoon, K Chung, R E Dick, D J Lege, F Pourboghrat, S-H Choi, and E Chu 2003 *International Journal of Plasticity* **19** 1297–1319
[4] F Yoshida, H Hamasaki, and T Uemori 2013 *International Journal of Plasticity* **45** 119–39
[5] H J Batista Alves, T Reis de Oliveira and C G Schön 2017 *Conference paper ESSC & Duplex*
[6] L R Treloar 2005 *The Physics of Rubber Elasticity*, 3rd ed. OUP Oxford
[7] D Banabic 2018 *Sheet Metal Forming Processes: Constitutive Modelling and Numerical Simulation* Springer
[8] J H Hollomon 1945 *Transactions of the Metallurgical Society of AIME* **162** 268–90
[9] R M Hackett, 2018 *Hyperelasticity Primer*. Springer International Publishing
[10] R S Rivlin 1948 *Philosophical Transactions of the Royal Society of London. Series A, Mathematical and Physical Sciences* **240** 459–90
[11] G Gruben, D Morin, M Langseth, and O S Hopperstad 2017 *European Journal of Mechanics A/Solids* **61** 315–29
[12] K Zhang, B Holmedal, O S Hopperstad, and S Dumoulin, 2014 *Materials Science Forum* **794** 596–601
[13] M Abspoel, M E Scholting, M Lansbergen, Y An, and H Vegte 2017 *Journal of Materials Processing Technology* **248** 161–177
[14] R Elleuch, K Elleuch, B Salah, and H Zahouani 2007 *Materials & Design* **28** 824–30